JOURNAL OF CATALYSIS 86, 427–432 (1984)

NOTES

Pore Structure of Catalyst and Intraparticle Diffusion of Gas

The pore structure of most catalysts are not entirely clear (*1*), and various models have been proposed to represent them. However, few models containing only micropores permit the calculation of diffusion rates in porous catalysts such as those based on alumina or silica. The present paper reports a model from which diffusion rates can be calculated. In this model, the pore structure is the space between an assembly of elementary spherical particles (*2*). The holes bounded by the elementary particles are connected to each other by narrow openings, called "pore neck" (*3*). The nature of such pore structure has reported by Higuchi *et al.* (*2*).

The effective diffusion coefficients D_e are evaluated in such porous bodies for the cases in which the elementary particles have the following packings: cubic close packed (CP), body centered cubic (BC), simple cubic (SC), and packing of the diamond type (DP). These types of packing are taken as typical of what one might find in porous bodies. The characteristics of the pore structures and the pore necks are summarized in Table 1 and Fig. 1.

Opening fraction $\theta°$ and path factor L, D_e can be obtained from the diffusion coefficient in pore D by means of

$$D_e = (\theta°/L)D, \qquad (1)$$

where $\theta°$ is the cross-sectional area of the pores per unit area of porous support in the plane normal to the direction of the diffusion in the pore, and L is the ratio of the length of tortuous diffusion path to the straight line path.

For the purpose of evaluation of $\theta°$ and L, the pore structure and the path may be approximated by use of the following assumptions: (a) The diffusion path between the holes is a straight line and the direction of the line can change at the center of a hole.

TABLE 1

Geometrical Characteristics for Each Type Packing Model (per Unit Cell)

	Packing type			
	CP	BC	SC	DP
Coordination number	12	8	6	4
Number of packed spheres	4	2	1	8
Lattice constant, l_1[a]	$2\sqrt{2}R_0$[b]	$4R_0/\sqrt{3}$	$2R_0$	$8R_0/\sqrt{3}$
Cross-sectional area, A_1[a]	$8R_0^2$	$5.333R_0^2$	$4R_0^2$	$21.33R_0^2$
Unit cell volume, V	$22.63R_0^3$	$12.32R_0^3$	$8R_0^3$	$98.54R_0^3$
Number of holes, n	Tetrahedral hole 8 Octahedral hole 4	6	1	8
Interval between holes, λ	$\sqrt{6}R_0/2$	$2R_0/\sqrt{3}$	$2R_0$	$2R_0$
Cross-sectional area of pore neck, A_n	$0.1612R_0^2$	$0.2437R_0^2$	$0.8584R_0^2$	$3.109R_0^2$
Void fraction, ε	0.2595	0.3198	0.4764	0.6599
$\varepsilon/(1-\varepsilon)$	0.3504	0.4702	0.9099	1.940

[a] Terms l_1 and A_1 show the value for (100) plane.
[b] R_0 is radius of elementary sphere packed.

0021-9517/84 $3.00

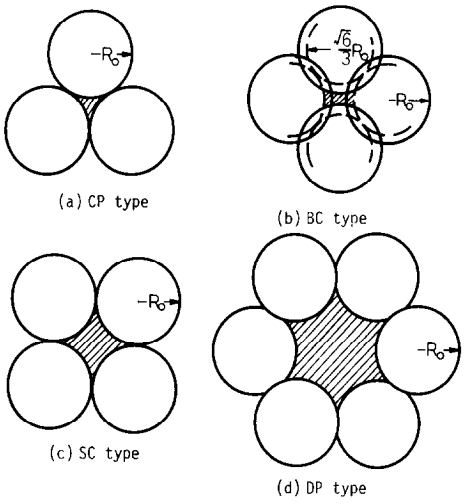

FIG. 1. Pore necks.

This path is designated a "flux line." The flux lines pass through all of the holes. Each series of holes contains only one flux line. But, exceptionally, a bigger hole (octahedral hole) is traversed by two flux lines in material with CP packing because there are twice as many of the smaller ones (tetrahedral holes) as of the larger ones. (b) Mass transfer is considered to be restricted at the pore neck. Thus, the effective size of a pore is assumed to be equal to the cross section of the pore neck (*4*). Namely, a flux line is assumed to have a uniform radius. (c) As a crystallographic plane of any of the various packings can be oriented in any direction, values of θ° or L are evaluated for the directions of diffusion normal to the (100), (110), and (111) planes. θ°/L is then obtained as an average of these three values.

Let n represent the number of holes in a unit cell, λ, a distance between centers of holes, and A_n, the cross-sectional area of flux line. Then, λA_n is the volume of a flux line in a hole and $n\lambda A_n$ is the total flux volume in a unit cell and is proportional to the void fraction of the porous body ε. For each packing model one can determine the area of a cell normal to the bulk direction of diffusion A_i and the distance to its direction l_i so that the volume of a unit cell is $V = A_i l_i$. If f is the number of lattice planes and n' is the number of holes on each plane in a cell, $n = n'f$. Thus, the following equation follows.

$$\frac{n\lambda A_n}{V} = \frac{n'A_n}{A_i} \cdot \frac{f\lambda}{l_i} = \theta^\circ L = k\varepsilon, \qquad (2)$$

$$\theta^\circ = n'A_n/A_i, \qquad L = f\lambda/l_i, \qquad (3)$$

where, k is a constant and n' is equal to the number of the diffusion fluxes. The calculated values are summarized in Table 2.

Applications. Figure 2 shows the calculated values of θ°/L plotted against $\varepsilon/(1-\varepsilon)$. When ε is less than that in the CP packing type, θ°/L is approximately proportional to the ε. We call this graph the "θ°/L diagram." It should be noted that this correlation is very useful for evaluating D_e.

The suitability of θ°/L can be seen by a comparison with experimental values for the intraparticle diffusion coefficients of Vycor glass and alumina samples which are considered to be the CP type (*5, 6*) and the SC type (*7*), respectively. That is, the experimental value for Vycor glass is 0.048–0.083 and for the alumina is 0.114–0.126. These experimental values agree with the calculated values.

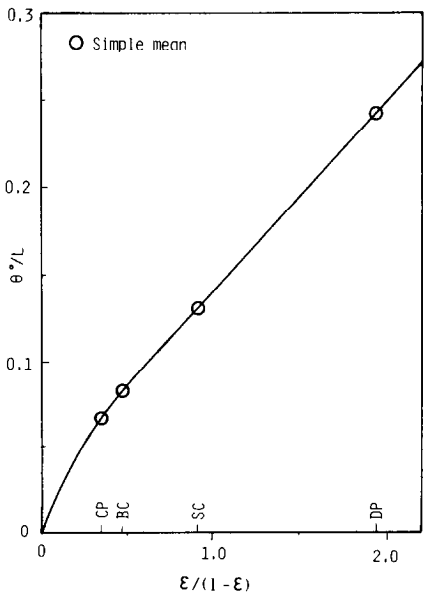

FIG. 2. Relationship between θ°/L and $\varepsilon/(1-\varepsilon)$, "$\theta^\circ/L$ diagram."

TABLE 2

θ°/L for Each Type Packing Model

Packing type	Plane	A_i	l_i	$n' = n/f$	$\theta^\circ = A_n n'/A_i$	$L = \lambda f/l_i$	θ°/L
CP	(100)	A_1	l_1	$4(n = 16)^a$	0.0806	$\sqrt{3}$	0.0465
	(110)	$\sqrt{2}A_1$	$l_1/\sqrt{2}$	8	0.1140	$\sqrt{6}/2$	0.0931
	(111)	$\sqrt{3}A_1$	$l_1/\sqrt{3}$	8	0.0931	3/2	0.0620
	Simple mean				($k = 0.538$)		0.0672
BC	(100)	A_1	l_1	$3(n = 6)$	0.1371	1	0.1371
	(110)	$\sqrt{2}A_1$	$l_1/\sqrt{2}$	3	0.0969	$\sqrt{2}$	0.0685
	(111)	$\sqrt{3}A_1$	$l_1/\sqrt{3}$	3	0.0792	$\sqrt{3}$	0.0457
	Simple mean				($k = 0.429$)		0.0838
SC	(100)	A_1	l_1	$1(n = 1)$	0.2146	1	0.2146
	(110)	$\sqrt{2}A_1$	$l_1/\sqrt{2}$	1	0.1517	$\sqrt{2}$	0.1073
	(111)	$\sqrt{3}A_1$	$l_1/\sqrt{3}$	1	0.1239	$\sqrt{3}$	0.0715
	Simple mean				($k = 0.451$)		0.1311
DP	(100)	A_1	l_1	$2(n = 8)$	0.2915	$\sqrt{3}$	0.1683
	(110)	$\sqrt{2}A_1$	$l_1/\sqrt{2}$	4	0.4122	$\sqrt{6}/2$	0.3365
	(111)	$\sqrt{3}A_1$	$l_1/\sqrt{3}$	4	0.3366	3/2	0.2244
	Simple mean				($k = 0.765$)		0.2431

[a] The $n = 16$ was obtained by 8 of tetrahedral holes and 4 of octahedral holes counted twofold.

EXPERIMENT AND DISCUSSION

Pore size distributions of catalysts. The γ-aluminas employed were Neobead C-5 (Mizusawa Kagaku), KH-D24 (Sumitomo Kagaku), Pechiney active alumina (Gaschro Kogyo), ACBM-1 and ACBR-3 (Shokubai Kasei), and the active carbons were Sx and HGH-620 (Takeda Yakuhin). The pore size distribution curves and pore volumes were determined by sorption isotherms (with a spring balance) of benzene at 0°C (*2*) for pores less than 18 nm in radius, and by the mercury porosimeter (Aminco No. 5-7118) for ones larger than 18 nm. The results are shown in Table 3 and Fig. 3.

Measurement of diffusion rate. Countercurrent diffusion rates of He and Ar through porous materials were measured under the constant pressures of up to 7 atm at room temperature by an apparatus of the Wicke–Kallenbach type. The diffusion rate of helium was determined by a calibrated thermal conductivity cell (Shimazu Seisa-

TABLE 3

Some Properties of Catalyst Pellet

Catalyst	Surface area (m^2/g)	Density ρ_p (kg/m^3)	Void fraction ε	Micropore, nm		Macropore, nm		Gas	$\frac{\sigma}{r_i}$	$\left(\frac{\theta^\circ}{L}\right)_i$	$\left(\frac{\theta^\circ}{L}\right)_a$
				ε_i	r_i	ε_a	r_a				
Neobead C-5	163	1520	0.552	0.552	3.9	0	—	He	0.065	0.119	
KH-D24	316	1390	0.590	0.505	1.9	0.085	189	He	0.13	0.117	0.022
Pechiney	293	1300	0.617	0.517	2.1	0.100	203	He	0.12	0.123	0.026
ACBM-1	170	760	0.791	0.448	4.3	0.343	50.2	He	0.06	0.109	0.090
ACBR-3	135	1340	0.613	0.430	3.5	0.183	52.2	He	0.07	0.102	0.047
Sx	826	689	0.649	0.374	1.2	0.275	2380	He	0.21	0.070	0.071
HGH-620	807	747	0.597	0.403	1.2	0.194	1490	He	0.21	0.076	0.050

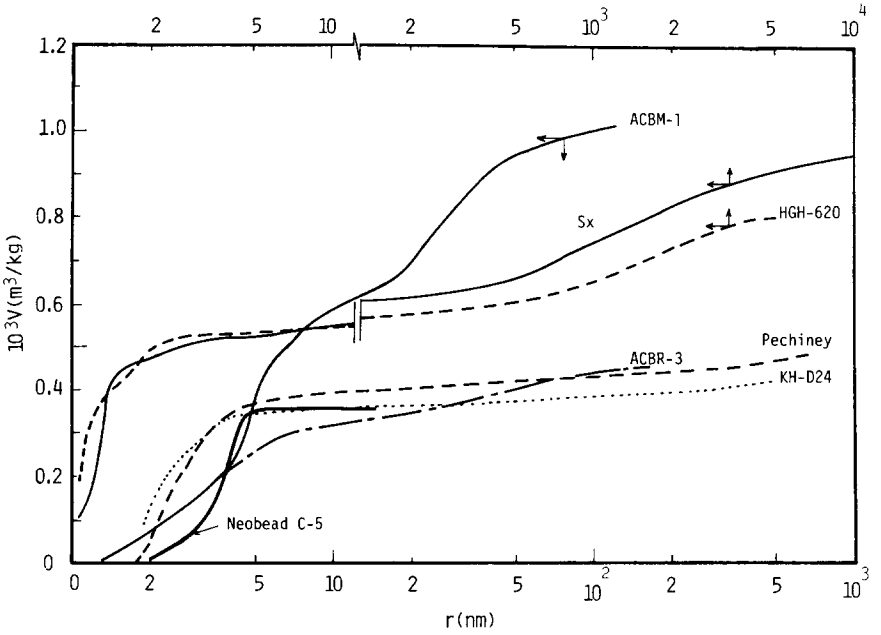

FIG. 3. Pore size distribution.

kusho, GC-3Ah, Active carbon packed). The effective diffusion coefficients D_e(exp) are shown in Fig. 4.

The rate of ethanol dehydration. The γ-alumina catalysts were employed for ethanol dehydration. The aluminas pelleted as spheres of 3.3 to 6.7 mm in diameter were designated as "large" catalysts. Powdered granules were prepared by crushing the pellets. They had an average of 0.089 mm (150/200 mesh) or 0.178 (65/100 mesh) and were designated as "small" catalysts. These catalysts were calcined at 450°C for 2 hr and the pore structures are shown in Table 3 and Fig. 3.

The ethanol was supplied from a microfeeder, and its vapor was fed to the reactor at a constant rate. The catalyst, 0.1 to 0.2 g, was packed in the reactor as a fixed bed. The water and unreacted ethanol which issued from the reactor were trapped by dry ice–methanol, leaving ethylene as the only untrapped product. Reaction rates were measured at 350 to 410°C. At this temperature, it was confirmed by gas chromatograph that only the products were ethylene and water. Conversions were obtained from ethylene formation rates. The kinetics were confirmed experimentally on small catalyst to be first-order in ethanol.

Evaluations of θ°/L and D_e in a bimodal pore structure. The evaluation of D_e by θ°/L was also tested for a bimodal pore structure. Most pelleted catalysts used in prac-

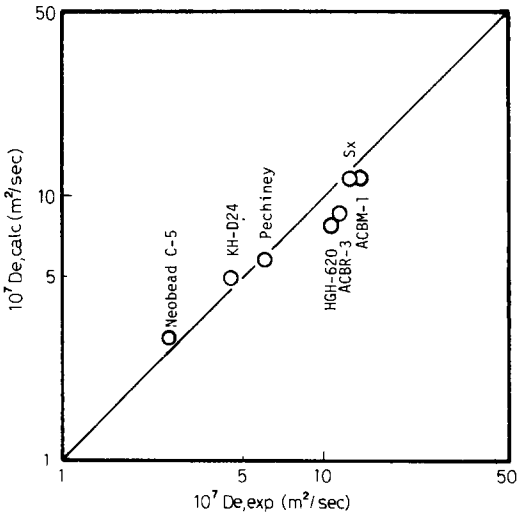

FIG. 4. Comparison of the experimental value D_e(exp) and the theoretical value D_e(calc) of effective diffusion coefficient of He at 7 atm (He/Ar at 25°C).

tice have a structure consisting of packed small microporous assemblies of particles. The spaces among these assemblies may be considered as macropores. Thus, the mass transfer in macropores may be evaluated from θ°/L diagram. The correction factor for micropores $(\theta^\circ/L)_i$ or for macropores $(\theta^\circ/L)_a$ was estimated from the void fractions ε_i or ε_a. Here, the interaction between micropores and macropores in diffusion was ignored. The diffusion rate N_1 was calculated by the equation:

$$N_{1i,a} = \frac{c_0 A D_{12}}{\alpha l_0} \left(\frac{\theta^\circ}{L}\right)_{i,a} \cdot \ln \frac{1 - \alpha y_{1,out} + (D_{12}/D_{K1i,a})}{1 - \alpha y_{1,in} + (D_{12}/D_{K1i,a})}, \quad (4)$$

$$N_1 = N_{1i} + N_{1a}, \quad (5)$$

where N_{1i}, N_{1a} = diffusion rate for micropores or macropores, A, l_0 = area or length of pellet, c_0 = gas concentration, $y_{1,in}$, $y_{1,out}$ = mole fraction of component 1 at the entrance or the outlet, $\alpha = 1 + N_1/N_2$ and D_{K1i},

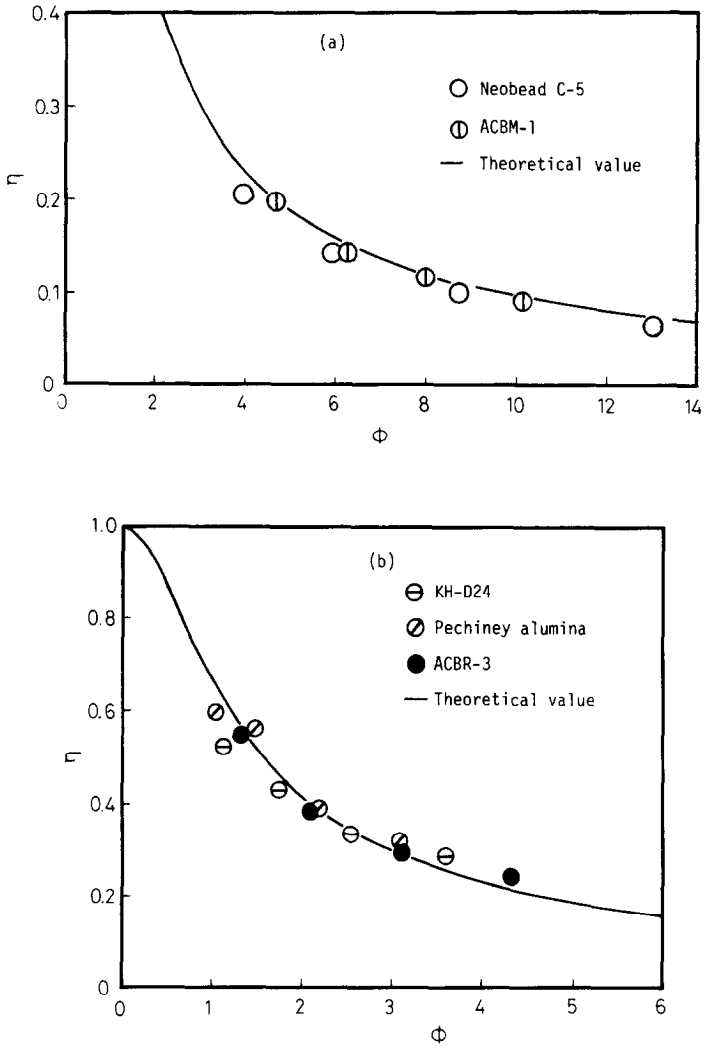

FIG. 5. Relation between theoretical or experimental effectiveness factor η and Thiele modulus $\phi = R_c\sqrt{k_s \rho_p RT/D_e}/3$ for dehydration of ethanol (first-order, spherical pellet).

D_{Kia} = Knudsen diffusion coefficients for the pore radii r_i for micropores and r_a for macropores. When the distribution of macropore $f(r)$ was broad, Eq. (4) was replaced by the equation:

$$N_{1a} = \frac{c_0 A D_{12}}{\alpha l_0} \cdot \frac{(\theta^\circ/L)_a}{\int f(r)dr} \cdot \int \ln \frac{1 - \alpha y_{1,out} + (D_{12}/D_{K1a})}{1 - \alpha y_{1,in} + (D_{12}/D_{K1a})} f(r)dr. \quad (6)$$

In the case of ε_i, it was better to use the void fraction which neglected the volume corresponding to micropore with less than several Ångstroms in radius. The effect of the size of the diffusing molecule (diameter = σ) was geometrically estimated by a factor $\{(r_i - \sigma/2)/r_i\}^3$, because the effective cross-sectional area of a pore decreases by a factor $\{(r_i - \sigma/2)/r_i\}^2$ and Knudsen diffusion coefficient was also decreased by $(r_i - \sigma/2)$.

In Fig. 4, the calculated values D_e(calc) are shown in comparison with the experimental results D_e(exp) at 7 atm. These D_e(calc) are in good agreement with D_e(exp).

Experimental effectiveness factor η_{exp} and the Thiele modulus ϕ. The η_{exp} was obtained by dividing the rate constant on a large catalyst k_L by that on a small catalyst k_S. The ϕ was obtained as $\phi = R_e\sqrt{\rho_p k_S RT/D_e}/3$, where R_e is the radius of the catalyst pellet and D_e is the calculated value. In Fig. 5, the theoretical relation between η and ϕ (*8*) is denoted by a solid line, and the experimental one between η_{exp} and ϕ is plotted. These experimental relationships are in reasonably good agreement with the theoretical curves.

These results shows that the packing structure model of elementary particles and the θ°/L method may be used as the basis for evaluating the diffusion coefficient of a catalyst pellet not only in monomodal pore structure but also in bimodal one.

ACKNOWLEDGMENT

This is contributed from D. Eng. dissertation by H. Katsuzawa, 1979, Chem. Eng. Dept., Tohoku University, Sendai, Japan.

REFERENCES

1. Everett, D. H., "The Structure and Properties of Porous Materials," Vol. X of the Colston Papers, p. 95, Butterworth, London, 1958.
2. Higuchi, I., Ushiki, Y., and Suzuki, R., *Nippon Kagaku Zasshi* **82,** *1620 (1961);* **83,** 808 (1962).
3. Higuchi, I., Kobayashi, J., and Katsuzawa, H., *Nippon Kagaku Zasshi* **90,** 150 (1969).
4. Katsuzawa, H., Sei, K., Shimura, M., and Kobayashi, J., *Nippon Kagaku Kaishi* **1976,** 512.
5. Kubota, S., Oda, H., and Higuchi, I., *Nippon Kagaku Zasshi* **88,** 43 (1967).
6. Raja Rao, M., and Smith, J. M., *AIChE J.* **10,** 293 (1964).
7. Katsuzawa, H., Kobayashi, J., and Higuchi, I., *Nippon Kagaku Kaishi* **1974,** 27.
8. Wheeler, A., "Advances in Catalysis," Vol. 3, p. 249. Academic Press, New York, 1951.

HIDEO KATSUZAWA

Department of Industrial Chemistry
Numazu College of Technology, Numazu 410, Japan

JUN-ICHI KOBAYASHI

Department of Synthetic Chemistry
Faculty of Engineering
Shizuoka University, Hamamatsu 432, Japan

Received October 28, 1982; revised November 22, 1983